Available online at www.sciencedirect.com
SCIENCE DIRECT®
Journal of Luminescence 101 (2003) 195–210
JOURNAL OF LUMINESCENCE
www.elsevier.com/locate/jlumin

Thermoluminescence spectroscopy of Eu^{2+} and Mn^{2+} doped $BaMgAl_{10}O_{17}$

T. Jüstel[a,*], H. Lade[a], W. Mayr[a], A. Meijerink[b], D.U. Wiechert[a]

[a] *Philips GmbH Forschungslaboratorien, Weisshausstr. 2, 52066 Aachen, Germany*
[b] *University of Utrecht, Princetonplein 5, 3584 CC Utrecht, The Netherlands*

Received 10 January 2002; received in revised form 7 August 2002; accepted 7 August 2002

Abstract

Thermoluminescence (TL) studies of Eu^{2+} and Mn^{2+} doped $BaMgAl_{10}O_{17}$ (BAM) are reported and discussed. The TL spectra that are measured after irradiation with ultraviolet (120–350 nm) show a series of TL peaks between 100 and 300 K. The TL spectra are similar for BAM with the two dopants, which suggest that the shallow traps are typical for the BAM host lattice. Using the Hoogstraaten analysis trap depths between 0.1 and 0.2 eV are determined. A model is proposed based on thermally activated recombination in local TL centres (not via the conduction band). Further support for this model is obtained from the observation that the TL signal is strongest for excitation around the band edge of BAM ($\sim$180 nm). Upon heating the samples in air all low temperature TL peaks decrease in intensity. In addition a new peak appears in the TL spectrum, which is connected with a deeper trap (0.3 eV) and also a partial oxidation of Eu^{2+} to Eu^{3+} is observed. The luminescence efficiency is lower and the UV induced degradation is faster after annealing in air. These results indicate that the shallow traps are related to oxygen vacancies. The shallow traps do not have a negative influence on performance (efficiency and degradation) of BAM as a lighting phosphor. The luminescence efficiency and stability are strongly influenced by the formation of Eu^{3+} and a deeper trap during annealing in air. Subsequent annealing in a reducing atmosphere restores the original properties.

Keywords: Thermoluminescence; Eu^{2+}; Mn^{2+}; $BaMgAl_{10}O_{17}$

1. Introduction

The doping of $BaMgAl_{10}O_{17}$ (BAM) with Eu^{2+} or Mn^{2+} yields highly efficient luminescent materials, which are widely employed as phosphors in plasma display panels (PDPs), Hg low pressure, and Xe low-pressure discharge lamps. Under photoexcitation BAM:Eu shows a single emission band at 453 nm, whereas BAM:Mn emits at 515 nm. Since BAM:Eu has a deep blue colour point, a short decay time ($\tau_{1/e} = 800$ ns) and a high efficiency under vacuum ultraviolet (VUV) excitation, it is applied as the standard blue phosphor in PDPs by all PDP manufacturers.

A considerable shortcoming of BAM:Eu is its sensitivity towards elevated temperatures. The degree of thermal degradation is dependent on annealing conditions, i.e. temperature and atmosphere [1–3], whereby the detected reduction in light output is a sensitive function of the excitation wavelength [1]. Moreover, the thermal stability of a given BAM:Eu powder is strongly determined by

*Corresponding author.

0022-2313/02/$ - see front matter
PII: S0022-2313(02)00413-1

its synthesis conditions, viz. appropriate weigh-in of starting materials and annealing temperature [4].

Additionally, BAM:Eu shows a severe degradation under VUV excitation, as it occurs in Xe discharge lamps and PDPs. Since its VUV degradation is much stronger than that of standard green- and red-emitting phosphors, i.e. $(Y, Gd)BO_3$: Eu and Zn_2SiO_4: Mn, used in these devices, the blue light intensity of lamps and displays is reduced over lifetime and the white colour point becomes more yellowish. This can be recognised as colour point shift of fluorescent lamps or as burn-in of plasma display panels. It was found that the photodegradation of BAM can be reduced by the optimisation of its composition [5].

Although BAM-based phosphors are used in lamps and displays and degradation and afterglow are a matter of concern for all device manufacturers, the type and density of defects in BAM are less known. This is surprising since lattice defects, in particular oxygen vacancies, can act as electron traps and therefore force the photooxidation of the unstable activators Eu^{2+} and Mn^{2+}. It can be expected that the crystallinity or defect concentration of BAM will strongly influence the stability of BAM and the luminescence properties.

The aim of this work is to gain insight in the influence of defects on the luminescence properties and to study the nature of the defects created under UV and VUV radiation by performing thermoluminescence measurements.

In addition, the effect of annealing of BAM:Eu in a reducing or oxidising atmosphere on the defect structure and density is investigated. Finally, the influence of the Eu^{2+} concentration and the behaviour of Mn^{2+} doped BAM is investigated.

2. Thermoluminescence fundamentals

Luminescence is the emission of light beyond thermal equilibrium, subsequently occurring after absorption of energy from an external source. In general it is distinguished between fluorescence, phosphorescence, and afterglow. While fluorescence is a fast process (ns to a few μs) based on a spin-allowed transition, the term phosphorescence is used if the emission process is based on a spin-forbidden transition, resulting in a long lifetime (typically ms to s). Afterglow is observed if the emission process is delayed by a transition into and out of a metastable level (also called a trap). The system remains in the metastable level until it receives sufficient (thermal) energy to return to the excited state followed by the recombination process associated with the emission of a photon.

Thermoluminescence and afterglow are caused by the same physical process. However, the first phenomenon is observed if a luminescent material is thermally activated due to the application of a temperature ramp. For that reason thermoluminescence (TL) is also called thermally stimulated luminescence (TSL).

For the fundamental discussion and analysis of thermoluminescence processes the reader is referred to the literature e.g. [6].

2.1. First-order kinetics (slow retrapping)

The thermoluminescence intensity $I_{TL}(T)$ of a given system at an arbitrary temperature rising rate $\beta = dT/dt$ is given by the Randall–Wilkens first order kinetics expression [7,8].

$$I_{TL}(T) = n_0 s \exp\{-E/kT\} \times \exp\left[-(s/\beta)\int_{T_0}^{T} \exp\{-E/k\theta\}\, d\theta\right]. \quad (1)$$

Here n_0 is the number of trapped electrons at the initial temperature T_0, E is the trap depth energy and k the Boltzmann factor, respectively. The meaning of the pre-exponential factor s is the so-called "attempt-to-escape frequency" [6], but the analysis and therefore its quantitative interpretation is not simple and depends strongly on the model and the assumed kinetic order [6]. That means if the excited state is a delocalised band (e.g. conduction band for electrons) the frequency factor can be related to vibrational frequencies of the trapped charge carrier, the effective density of states in the delocalised band and the free carrier thermal velocity [9]. Since all individual features are temperature dependent, so s also exhibits temperature dependence. Fortunately, s varies slowly with temperature [10] and is often kept in

the analysis constant for a particular TL peak for simplicity reasons.

With increasing temperature I_{TL} increases as the second exponential term in Eq. (1) approximates unity, reaches a maximum and falls off for further increase of temperature as the second exponential decreases rapidly to reduce I_{TL} to zero.

A typical feature of a glow curve is the asymmetry of the peak, i.e. it has a more pronounced tailing on the low temperature side than on the high temperature side. With increasing trap depth E the peak shifts to higher temperatures, along with a decrease in the height and an increase in the width (keeping the area constant).

By increasing the heating rate β, the peak shifts to higher temperatures and the intensity of the peak increases. Note that the peak area on this temperature axis scales with β, but if plotted as a function of time the area would remain the same as the heating rate changes.

2.2. Higher-order kinetics

The second-order kinetics will be exhibited by those materials in which the concentration of traps and recombination centres are almost equal. For larger concentrations of recombination centres the observed glow curves will follow first-order kinetics. For intermediate concentration relations the general order kinetics can be applied, but this is accompanied by the disadvantages discussed above.

The analysis described above relies on the simple one-trap/one-centre model. Most luminescent materials, however, comprise several types of traps or trap systems. In particular, if there exist deep traps which retain their trapped electron population during emptying of the shallower traps (read-out of the TL signal), the kinetics of the complete system becomes much more complicated. Depending on special assumptions, it can be distinguished between interactive and non-interactive kinetics of multiple trapping and/or recombination states. The theory of this detailed discussion is beyond the scope of this report and more details are described elsewhere [6].

Finally, one aspect should be noted if a multiple trap system is investigated: depending on the actual trap density, different kinetics for shallow traps and deep traps are possible. At low temperatures the shallow traps are read out and the deeper traps may partly trap the released electrons—typical second-order kinetics may result. Further increase of temperature results also in a read out of the deeper traps but the released electrons now cannot be retrapped by the shallower traps due to the higher temperature—resulting in a typical first-order kinetic behaviour. Therefore, for glow curves with different TL-peaks the shape of the individual peaks may differ.

2.3. Analysis of TL glow curves

Any model of thermoluminescence includes a number of parameters, which are physically rather interesting in relation to the trapping state responsible for the TL emission. In the field of TL spectroscopy typically the glow curve features are analysed with respect to a model selected on base of a set of assumptions, e.g. kinetic order, number of luminescence centres and traps and their possible interaction etc. For a detailed review of more than 30 different methods published in the literature so far the reader is referred to Kivits and Hagebeuk [11]. In Ref. [11] the authors also applied several methods to numerically calculated TL and TSC curves and compared their reliability.

The method that delivers the most reliable results in terms of trap depth energy [11] is the method of various heating rates, which will be applied in our own experiments.

2.3.1. Method of tuning the heating rate

By changing the heating function or even changing the heating rate (linear heating function), the shape of the TL peak and thus the temperature with the maximum TL intensity T_m will be altered.

Looking for the temperature of maximum TL intensity T_m, one yields for first-order kinetic processes from Eq. (1) and the setting of $dI_{TL}/dT = 0$ at $T = T_m$:

$$\frac{\beta \cdot E}{kT_m^2} = s \exp\{-E/kT_m\}. \quad (2)$$

In Ref. [12] Hoogenstraaten proposed the use of several linear heating rates. From Eq. (2) it is

obvious that a plot of $\ln(T_m^2/\beta)$ vs. $1/T_m$ yields a straight line with the slope of E/k and an intercept at $1/T_m \to 0$ of $\ln(E/sk)$ from which E and s can be easily deduced.

Note an inherent problem of this method. In a full-scale plot experimental data typically exists only within a very small region, far away from the intersection point. Furthermore, the frequency factor is exponentially related to the glow curve data. Both facts, i.e. the large extrapolation range and the exponential interpretation, lead to a large uncertainty in the determination of the frequency factor s. Because the trap depth energy is directly related to the glow curve data and the uncertainty of the slope is fairly small the trap depth energy can be deduced with a reasonable accuracy.

Until now the discussion was restricted to first-order kinetics. In a more general discussion performed in Ref. [11] it is shown that for second-order kinetics, Eq. (2) is still valid if s is replaced by an effective frequency factor s_{eff}, given by $s_{eff} = (2a^+/h)s$, where a^+ is the hole concentration at the recombination centre at peak maximum temperature, h is the trap concentration and s the frequency factor formally discussed. This parameter is nearly a constant for a given trapping level.

While also for general-order kinetics [13] a plot of $\ln(T_m^2/\beta)$ vs. $1/T_m$ still yields a good value for E [10] from the slope of the line, the analysis of s, s_{eff}, or more general the interception in the plot, becomes difficult and its physical interpretation is troublesome and strongly related to the model assumptions.

In conclusion, multiple measurements performed with various heating rates in combination with the graphical analysing method supposed by Hoogenstraaten produces reliable values for the trap depth which are more or less independent of the values of the frequency factor and the retrapping ratio.

3. Experimental

3.1. Sample preparation

The reference BAM:Eu (U771) is a commercially available sample from Philips Lighting manufactured in Maarheeze, NL. All other BAM samples were made by a conventional solid-state synthesis using $BaCO_3$, MgO, MgF_2, Al_2O_3, $MnCO_3$, and Eu_2O_3 as starting materials. The materials were milled and subsequently annealed in a reducing atmosphere (5% H_2 in N_2) at 1250°C for 2 h. XRD analysis showed that the obtained powders are of single phase.

To ensure a good thermal conductivity thin powder layers were prepared on top of small stainless steel substrate plates by a simple sedimentation process in water without using a binder. All these layers had a thickness of about 50 μm.

3.2. Spectrometer set-up

The VUV spectrometer set-up used allows exciting phosphor samples from 115 to 350 nm. It consists of a Deuterium lamp, a vacuum monochromator and a refocusing. The VUV excitation unit is fully integrated into the spectrofluorimeter system FL900 of Edinburgh Instruments. The detection part of the spectrometer consists of a collecting optic, a monochromator and a photomultiplier tube (PMT) mounted in a Peltier cooled housing, whereby spectra are recorded by using the single photon counting technique. A detailed description of the set-up and its performance was recently given in [14].

For recording thermoluminescence spectra a variable temperature (VT) sample head was constructed, that allows the cooling and the heating of phosphor samples in a controlled manner.

In the VT head, liquid Nitrogen is pressed against the front end plate. Integrated in the front end plate is a resistive heater enabling a controlled heating of the sample. Additionally, a thermocouple (PT100) is incorporated in the front plate just below the surface, which delivers the adjustment signal for the active control unit for the resistive heater.

Starting at room temperature the asymptotic temperature value of −155°C is reached within 10–12 min.

The active control unit allows the heating of the sample with a linear ramp. With a starting temperature of −155°C and an end temperature

of 30°C ramping times down to 4 min can be chosen corresponding to a heating rate of 46 K/min. For ramping times below 4 min the thermal time constant of the set-up is to slow to follow the actively driven heater resulting in an increasing temperature difference between the temperature sensor and the surface of the sample which was carefully checked to be below ±2°C. In the measurements, care was taken that the long time ramping limit is mainly determined by the glow curve features and not by the hardware components. Heating rates below 10 K/min can be achieved.

3.3. Thermoluminescence measurements

Thermoluminescence spectra are obtained as follows. After mounting and adjustment of the sample, the liquid nitrogen valve is opened and the sample cools down to the minimum temperature within 10–12 min. During the cooling process the sample is permanently excited by VUV light. After reaching the lower temperature limit—which is the starting temperature for the thermoluminescence experiment—the liquid nitrogen valve is closed and the measurement of the thermoluminescence glow curve starts.

At the same time the linear ramp routine of the heater power supply is started, the excitation source is switched off and the kinetic measurement program is initiated. From this time on, the actual temperature is recorded as function of time.

For the trap analysis the glow curves are measured at different heating rates. This is done by successively repeating of the described measurement procedure with several linear ramp times.

Typically the sample is excited at around 160 nm that is the wavelength with the highest intensity of the spectrometer set-up [14]. It is important to note, that timing is such, that the sample is temporarily excited as close as possible to the acquisition of the glow curves. By doing so, the TL signals to be detected, are not reduced by TL decay at the (low) starting temperature. TL emission is always monitored at the wavelength where the maximum emission intensity of the respective phosphor is recorded.

4. Experimental results

4.1. Undoped BAM and BAM doped with Eu^{2+}

4.1.1. Luminescence spectra of BAM and BAM:Eu

$BaMgAl_{10}O_{17}$ (BAM) crystallises in the β-alumina structure [15] which is built up of spinel blocks spaced by the so-called conduction layers, comprising barium and oxygen ions. These Ba–O layers are analogue to the Na–O layers in $NaAl_{11}O_{19}$, which is one of the best ion conductors. The high ion conductivity is caused by the mobility of Na ions in the conduction layer which implies a relatively high defect density. Consequently, also BAM is expected to have many defects in the conduction layer. This is confirmed by the relatively efficient defect luminescence between 250 and 400 nm under VUV excitation. The observed defect related luminescence is most efficient if excitation occurs at 170 nm (Fig. 1), which is in line with the band edge of $BaMgAl_{10}O_{17}$ at about 7.0 eV.

If BAM is doped by the activator Eu^{2+}, which replaces Ba^{2+} in the conduction layer, it shows very efficient luminescence at 453 nm under photoexcitation with energies higher than 3.2 eV. The excitation spectrum (Fig. 1) reveals two broad bands at around 240 and 320 nm caused by Eu^{2+} centred transitions between the ground state $4f^7$

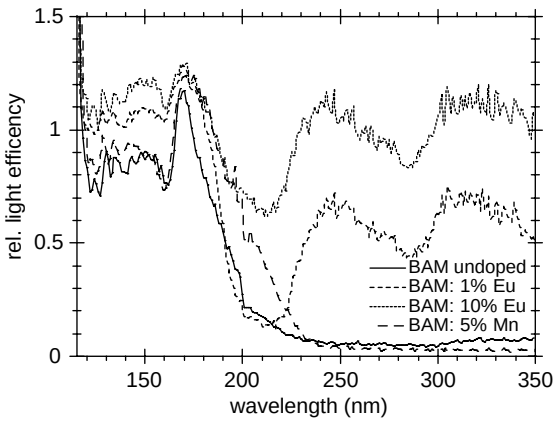

Fig. 1. Excitation spectra of BAM samples monitored at the maximum of the emission band (260 nm for undoped BAM, 453 nm for BAM:Eu, and 515 nm for BAM:Mn).

and the crystal-field split $4f^6 5d^1$ configuration. The assignment of these bands to Eu^{2+} centred transitions is in line with their intensity dependence on the activator concentration. The quantum efficiency below 180 nm, i.e. under exciton or band excitation, is almost unity [14], which is responsible for the wide application range of this phosphor.

4.1.2. Glow curves of BAM:Eu under 160 nm excitation

All investigations in this paragraph were performed on a commercial sample U771 from Philips Lighting. In Fig. 2 the measured TL intensity vs. temperature, i.e. the glow curve, for several heating rates, as labelled in the figure, is depicted. The time integrated TL intensity is similar for all these glow curves. It is reasonable to associate this area with a direct relation to the total number of TL photons and therefore to the total number of trapped electrons. Similar integral TL intensity for all heating rates means that during each run the same number of trapped electrons are released, indicating that prior to the heating period the density of trapped electrons is nearly identical. This proofs the reproducibility of the experimental procedure.

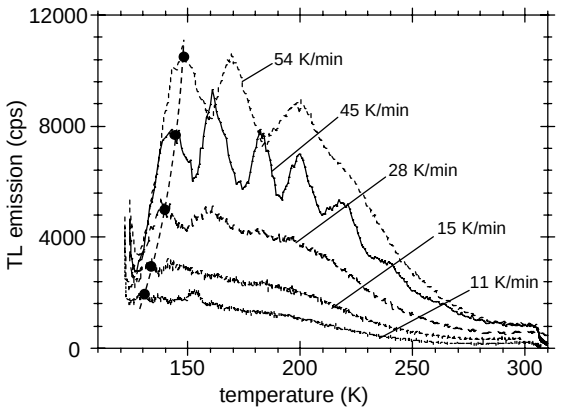

Fig. 2. TL glow curves of BAM:Eu (U771) under 160 nm excitation, monitored at 453 nm for several heating rates as labelled in the figure. The maximums of the first glow peak are indicated by thick dots and a visual fit given by the dashed curve.

Obviously the obtained glow curves are not simply shaped as single glow peaks, but consist of a superposition of several individual glow peaks, which strongly overlap in the wing regions. Only for certain heating rates the individual peaks become distinguishable. Such a fine structured glow curve shape suggests the existence of a multilevel trapping system which will be discussed later.

For further analysis the peak maximum of the first glow peak is indicated by thick dots in the figure for each glow curve. The dashed curve corresponds to a visual fit through all these first peak maxima.

The ''Hoogenstraaten'' graphical analysis of the individual glow peaks is depicted in Fig. 3. In this graph, the temperatures of the maxima of the individual glow peaks (for those separately identified) are incorporated. Data points corresponding to similar peaks are represented by similar symbols. The results of the graphical analysis in terms of trap depth energy E/k and frequency factor s are depicted in Fig. 3.

By the linear extrapolation of the data points, the uncertainty of the trap depth energy can be estimated to be about $\pm 20\%$. However, as discussed before, the uncertainty of determining the frequency factor can easily reach one order of magnitude.

In the measured glow curves up to six TL peaks can be separated. While the first TL-peak (low

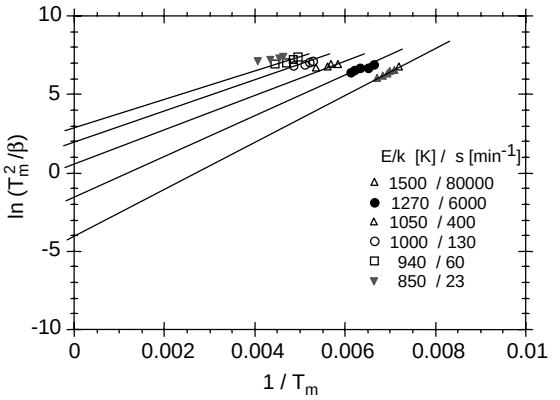

Fig. 3. The graphical analysis of the individual glow peaks T_{m1} denotes the glow peak temperature of the first occurring glow peak, T_{m2} the second one etc.

temperature peak) corresponds to a trap depth of $E/k = 1500$ K (~ 0.13 eV) the corresponding trap depth energy of the following glow peaks decrease successively down to ~ 850 K (~ 0.07 eV). In conclusion, the observed multiple peak structured glow curves suggest the existence of a multiple trap system with energetically well separated trapping levels.

By taking the obtained frequency factors into account, the interpretation becomes more difficult. The deeper the trap the higher the frequency factor is, which is a surprising observation. To understand this result one has to keep in mind that the complete analysis so far is based on the model of a single trap structure with a single recombination centre. Especially the first assumption—a single trap system—is obviously not valid in this material. For a multiple trap system (and multiple recombination centres) the interactive kinetics have to be considered. This easily leads to quite complicated considerations and is performed for different model assumptions in the literature by several authors, see e.g. Ref. [6].

The conclusion to be drawn from these considerations is, that in systems in which the recombination process dominates over the retrapping processes, the TL glow curve can be represented accurately by the superposition of individual first-order peaks of the Randall–Wilkens type. For systems in which appreciable retrapping is likely, the actual glow curve shape will show significant deviations from the superposition of second-order processes. Under these circumstances, analysis of the data based on simple equations, such as first-, second-, intermediate-, or mixed-order may prove to be unreliable.

The value of the effective frequency factor decreases generally with increasing retrapping phenomena [6]. Neglecting all the interpretation problems, which may occur due to the interactive kinetics of multiple trap systems, the obtained decrease of the effective frequency factor for smaller trap depths energies may be interpreted as an increase of the retrapping probability for shallower trap levels. This phenomenon may be easily explained assuming that the trapping centres are spatially close to each other. In this case, one must be aware of the possibility that the trapped charge wavefunctions may overlap to such an extent that tunnelling can occur between trap centres, leading to effective retrapping of the shallow traps into the energetic deeper trap states with higher frequency factors. However, it is still a peculiarity that the deepest traps show the highest frequency factors.

A second possible explanation for the obtained frequency factor—trap depth relation is based on a localised transition model for the traps. This model is also suggested by further experimental results described in the next section. Here the obtained decrease of the effective frequency factor for smaller trap depths will occur if the deeper traps are spatially closer to the recombination centre than the shallower ones.

In summary, the investigated BAM:Eu U771 batch shows strong thermoluminescence after VUV radiation exposure. The glow curve shows fine structure, consisting of a superposition of several individual glow peaks suggesting the existence of a multi level trap system. Neglecting all possible interactive kinetics an analysis based on individual first-order peaks reveals trap level energies between 0.07 and 0.13 eV. The obtained increase of the deduced frequency factor with increasing trap depth may be interpreted either as a trap level related retrapping probability due to spatially overlapping, trapped charge wavefunctions or by a localised transition model with trap depth related distances between the trap and the recombination centre.

4.1.3. Glow curves of reference BAM:Eu (U771) as function of the excitation energy

Until now the filling of the traps was performed by 160 nm radiation corresponding to an energy of 7.75 eV which is distinctly higher in energy than the band gap of BAM. For a detailed investigation of the multi trap level system obtained the thermoluminescence experiments have been repeated at several excitation wavelengths between 120 and 350 nm.

The shape of the TL glow curves is almost independent of the excitation energy. The pattern of the glow peaks appears in all glow curves with hardly any changes in peak temperatures.

The integrated measured thermoluminescence intensities—normalised to the actual excitation intensities—are shown in Fig. 4 by the dots with reference to the spectral excitation properties—the light output spectrum—of BAM:Eu.

The normalised TL intensity clearly reveals a peak at an energy close to the conduction band edge, viz. at about 180 nm. In addition to this resonant excitation of the multilevel trap system, it is still excited at higher energy, e.g. at 120 nm, which corresponds to excitation into higher states within the conduction band. Finally, also excitation with lower energy, between 200 and 350 nm, yields the population of the multilevel trap system. The latter observation implies on the one hand that the trapping levels can also be populated after an Eu^{2+} centred $4f^7$-$4f^6 5d^1$ excitation. On the other hand it is an indication that the electronic trap structure is based on localised transitions, which will be discussed later in more detail.

4.1.4. Glow curves of BAM:Eu as function of the Eu concentration

To evaluate the energetic structure of the multilevel trap system BAM samples have been prepared with Eu^{2+} concentrations between 1% and 25%. The glow curves of these materials were recorded with a heating rate of 38 K/min as depicted in Fig. 5.

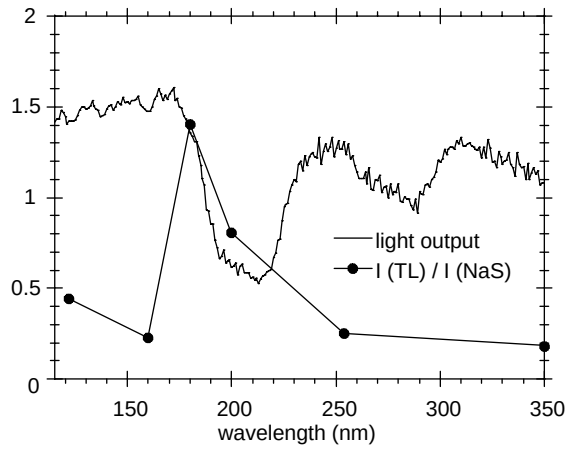

Fig. 4. Spectrally resolved light output of BAM:Eu U771 (solid line) and the measured TL-intensity I(TL) (dots) normalised to the applied excitation intensity I(NaS).

The glow curves obtained reveal that the pattern of the peaks is independent of the Eu concentration. The glow curve of the sample with 10% Eu prepared on lab scale is very similar to that of the reference BAM:Eu sample U771 which has the same composition in terms of Ba/Mg/Al ratio and Eu^{2+} concentration. This result implies that the observed density and energetic position of the traps present in BAM:Eu is dominated by its composition and not or to a lesser extent by the specific preparation process. In addition, these glow curves demonstrate that the TL intensity decreases with increasing Eu^{2+} concentration.

This behaviour can be explained either by an Eu^{2+} governed trap density variation or by the fact that for a given trap density the trapping probability is reduced if the density of the activator ion is increased due to the statistical reduced spatial distance between the activator ions and the excitons formed after band absorption.

4.1.5. Thermal cleaning of BAM:Eu glow curves

Further information on the energetic structure of the trap system can be gained from thermal cleaning experiments. In this experiment the electrons in a specific trap are released by a preheating step.

Here, glow curve recording is started as usual but after a linear heating ramp for 1 min, resulting

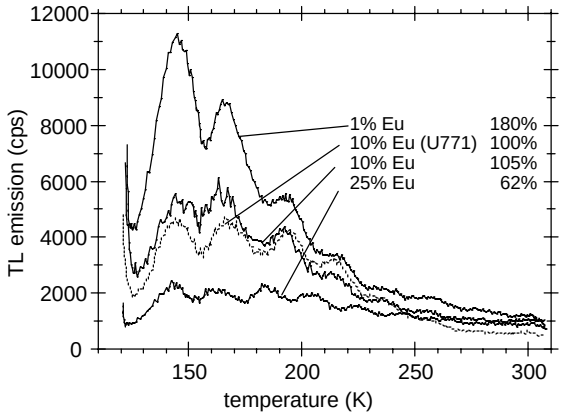

Fig. 5. TL glow curves of BAM:Eu samples as function of the Eu^{2+} concentration after 160 nm excitation monitored at 453 nm. The integrated TL intensities are related to the standard sample U771 (100%) and listed in the figure.

in a sample temperature of about −120°C, the heating process is terminated and the sample is cooled down again to −150°C within 3 min, but without additional VUV excitation. After 3 min holding the sample at this temperature, the linear heating ramp is started again and the glow curve is recorded.

Fig. 6 displays the glow curve obtained by this temperature cycle and compares it to the glow curve recorded without interrupting the heating process.

For all these cleaning experiments the time integral of the glow curves were found to be similar to the 'standard' TL runs, indicating negligible non-radiative loss mechanisms for the trapped states.

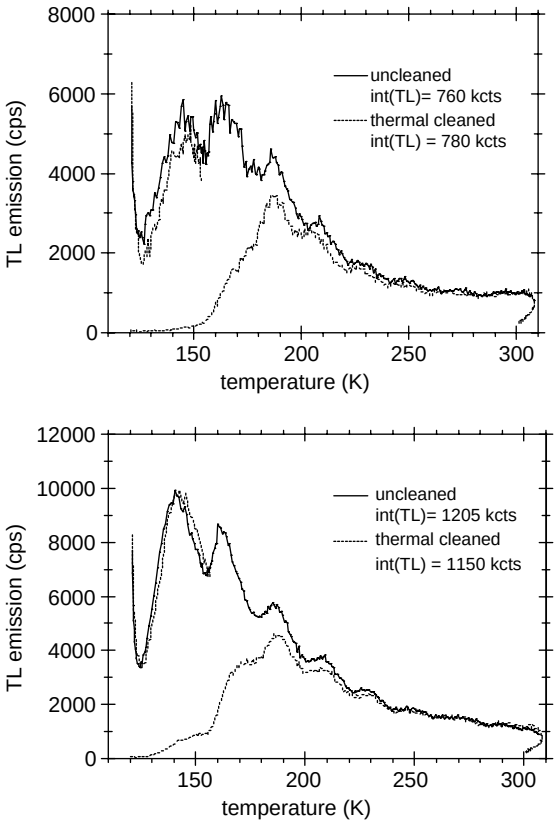

Fig. 6. TL glow curves of BAM doped with 10% Eu (top graph) and 1% Eu (bottom graph) without cleaning (solid lines) and with thermal cleaning (dashed lines). The heating rate is 38 K/min.

After the preheating run the very first glow curve peak, occurring at −130°C, is vanished in the second heating run (completely for the 10% Eu sample and largely for the 1% Eu sample) which means that the trap associated with this peak is completely empty due to the preheating procedure and is refilled by intra-trap relaxation processes for the 10% Eu sample but only partially for the 1% Eu sample.

All these observations are in line with spatially well separated trapping sites where the retrapping probability increases with the required average diffusion length of a released electron to the next recombination centre, i.e. to the activator Eu^{2+}. It can be assumed that those trapping sites, which are close to the Eu^{2+}, have a higher trap depth since they induce a larger distortion of the lattice, since they are located in the flexible conduction layers. The spatial proximity results in high frequency factors due to the larger overlap of the wave functions. In contrast, trapping sites far away from the recombination centre, i.e. in the spinel blocks, less distorts the host lattice, but also give smaller frequency factors due to the lower overlap of the wave functions.

4.2. BAM doped with Mn

BAM:Mn is considered as a green phosphor for PDPs due to its high VUV efficiency and excellent green colour point, however, most PDP manufacturers presently still apply Zn_2SiO_4: Mn due to its better VUV stability (Fig. 7).

In contrast to BAM:Eu, the activator Mn^{2+} substitutes Mg^{2+} and is thus incorporated into the spinel blocks instead into the conduction layers. The excitation spectrum of BAM:Mn (Fig. 1) is very similar to that of BAM, since Mn^{2+} has only forbidden transitions resulting in low absorption coefficients. The only difference to the undoped BAM is that the band edge is somewhat shifted towards lower energy, which is caused by the replacement of Mg^{2+} by Mn^{2+}.

The low temperature part of the glow curves of BAM:Mn are very similar to those of BAM:Eu (U771), indicating that the defect structure responsible for the complex glow curves are an intrinsic feature of the BAM host lattice,

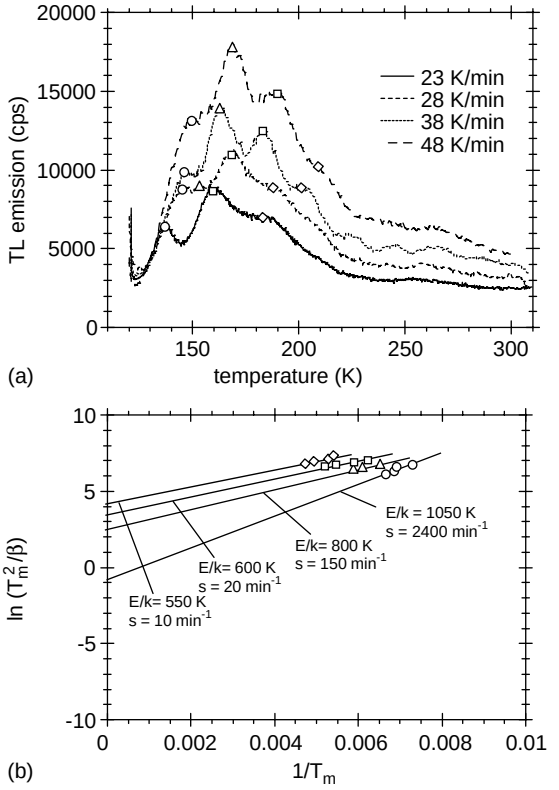

Fig. 7. TL glow curves of BAM:Mn 5% deduced with different heating rates (a) and the Hoogenstraten analysis plot (b) of the first four glow peaks marked (in top) by different symbols corresponding to different peaks. Similar symbols are used in (b).

independent on the type of dopant. However, the integral TL intensity of BAM:Mn is about twice as high as that of BAM:Eu. The analysis of the glow curves show that the activation energy of the shallow traps in BAM:Mn is about 0.04 eV ($E/k \sim 400$ K) smaller than of those in BAM:Eu.

The glow curves of BAM:Mn exhibit in the high temperature section an additional glow peak that is not present in the glow curves of BAM:Eu. This deep trap is thus ascribed to the incorporation of Mn^{2+} in the BAM lattice.

4.3. Thermal treatment of BAM:Eu in air (oxygen)

A major concern related to the application of BAM:Eu in PDP is the distinct reduction of its efficiency if it is annealed in an oxidising atmosphere, i.e. in air or in oxygen. This is a necessary step during the PDP manufacturing process [16] to remove organic matter, e.g. binder residues, from the screen-printing steps. The VUV efficiency is already reduced if the annealing temperature is above 300°C, while the efficiency under UV-C radiation only drops if the powder is heated above 600°C. Oshio [2] and we found that the reduction of the efficiency of BAM:Eu due to a thermal treatment above 600°C is related to the oxidation of the activator Eu^{2+} to its trivalent state. An annealing step in the temperature range 300–600°C only results in the reduction of the VUV efficiency, while the UV-C efficiency is maintained.

VUV excitation results in the formation of excitons that can be trapped either by the activator or by defect sites. While trapping of the excitons at the activator directly yields luminescence, trapping at defect sites does not result in the desired Eu^{2+} emission. It is thus expected that type and density of defects have an impact on the VUV efficiency of BAM:Eu.

To investigate the influence of a thermal treatment on intrinsic defects, with respect to depth and density, the TL properties of BAM:Eu U771 after annealing in various atmospheres and temperatures were investigated. The relative light output spectra of the untreated and the thermally treated reference BAM:Eu (U771) are shown in Fig. 8.

It is obvious that the light output of the phosphor is not affected by the thermal treatment in air for excitation energies below 7.0 eV (180 nm), i.e. for energies lower than the band gap of the host lattice. For higher photon energies the efficiency decreases steadily with increasing thermal treatment. The observed reduction of the light output for photoexcitation above the band gap becomes more pronounced with increasing photon energy. These results were interpreted in terms of the low penetration depth of VUV photons into the BAM grains [16].

Since VUV radiation is absorbed in the band gap with a very high absorption coefficient, the penetration depth of the incident photons is low. As a result the oxidation of Eu^{2+} to Eu^{3+} at

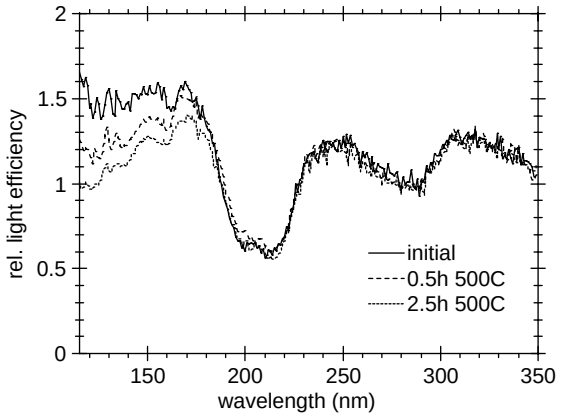

Fig. 8. Light output spectrum of the BAM:Eu U771 initially (solid line), after thermal treatment in air for 30 min at 500°C (dashed line) and after thermal treatment in air for 2.5 h at 500°C (dotted line).

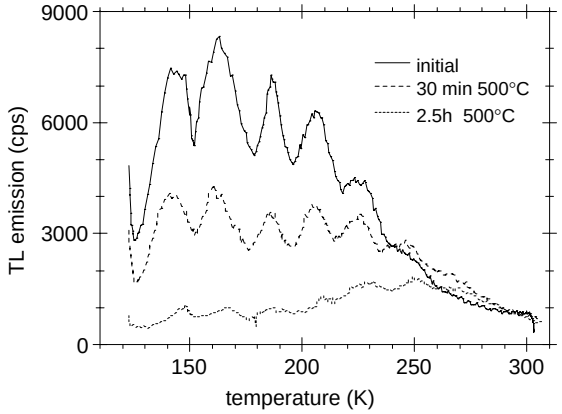

Fig. 9. Glow curves of BAM:Eu U771 recorded at a heating rate of 44 K/min, non-treated (solid line), after 30 min annealing in air at 500°C (dashed line), and after 2.5 h annealing in air at 500°C (dotted line).

the surface of the BAM:Eu particles can be monitored. Since Eu^{3+} is not blue luminescent, its thermal treatment in air yields a reduction of the VUV light output by the reduction of the concentration of luminescent Eu^{2+} centres in the surface layer. Alternatively, it can be ascribed to the energy transfer from Eu^{2+} to Eu^{3+} or to the trapping of excitons due to Eu^{3+}.

Under UV-C excitation the photons are absorbed due to the $4f^7$–$4f^6 5d^1$ transition of Eu^{2+} that have a lower absorption coefficient than host lattice absorption. Therefore, the oxidation of Eu^{2+} to Eu^{3+} in a thin surface layer hardly affects the excitation spectrum above 190 nm.

Here the question arose, whether the thermal treatment of BAM:Eu has an impact on its glow curves, i.e. on its defect density and structure. Therefore the TL-glow curves of BAM U771 have been measured after each thermal treatment step by exciting the samples at 160 nm (Fig. 9).

The glow curves of BAM:Eu as function of the applied annealing time show two distinct changes relative to the glow curve of non-treated BAM:Eu: On the one hand the intensity of the glow peaks related to the shallow traps decreases to such an extent that they almost disappear after an extended annealing period. On the other hand a high temperature trap shows up, whose intensity increases with increasing annealing time.

All observations concerning the glow curves of thermally treated BAM:Eu can be briefly summarised as follows:

(i) The glow curve fine structure, i.e. the superposition of several glow peaks, is still observed for thermally treated samples.
(ii) A detailed analysis of the individual TL-peaks reveals more or less similar results for the trap depths and the frequency factors. This indicates, that the trap energy levels are not altered by the thermal treatment in air.
(iii) The integral of the glow curves decreases with increasing treatment time for a similar heating rate. A heating rate of 54 K/min yields TL-peak intensity of ~10 000 cps for the starting material, which drops down to ~4500 and ~1000 cps after 0.5 and 2.5 h thermal treatment, respectively. This observation shows that the trap density of the multiple trap system decreases due to the thermal treatment in air. This implies that the multiple trap level system is not responsible for the observed decrease of the light output in the VUV range.
(iv) The high temperature TL peak due to the thermal treatment occurs at temperatures around 240 K. The Hoogstraaten analysis of this newly generated TL peak yields a trap

depth energy of $E/k = 3500$ K ($E \sim 0.3$ eV) and a frequency factor of $s \sim 65\,000$ s^{-1}.

4.4. Thermal annealing of BAM:Eu in Nitrogen

While the thermal treatment in an oxygen containing atmosphere yields a reduction of the light output of BAM:Eu under VUV excitation, the treatment in an oxygen free atmosphere, e.g. nitrogen or argon, does not reduce its VUV efficiency [16]. This is in line with the experience from the BAM:Eu production. After the removal of BAM:Eu from the furnace, in which it is annealed under nitrogen/hydrogen, which is required to reduce europium to its divalent state, it is stored under nitrogen until it has been cooled down to room temperature. To work out whether the annealing of BAM:Eu under nitrogen has an impact on its defect structure and density, TL glow curves were measured after 0.5 and 2.5 h annealing at 500°C under nitrogen, although such a treatment has hardly an impact on its VUV efficiency.

The thermal treatment experiments were performed on BAM:Eu U771 under similar conditions (same furnace) to the thermal treatment series in air. Therefore, the measured glow curves can be directly compared. In contrast to the thermal treatment in air, the treatment of BAM:Eu under nitrogen does not influence the light output of the phosphor material over a large wavelength range. A slight degradation of its light output is only observed for excitation below 140 nm. Similar to the thermal treatment series in air the TL-glow curves have been measured also after each treatment process in nitrogen atmosphere with identical measurement conditions to the air treatment series.

The features of the observed TL-glow curves can be summarised as follows:

(i) As already observed for the thermal treatment in air, the TL-fine structure, i.e. the superposition of several TL-glow peaks is still observed for the samples thermally treated in nitrogen. A detailed graphical analysis of the TL-peak maximums reveals more or less similar results for the trap depths and the frequency factors. This means that the trap energy levels remain unchanged.

(ii) Comparing the glow curves with similar heating rate the decrease of the TL-intensity with increasing treatment time is obvious. In contrast to the thermal treatment in air the TL-intensity reduction is smaller for the treatment in nitrogen. E.g. for a heating rate of 38 K/min, a TL-peak intensity of ~ 8000 cps is obtained for the initial material decreasing down to ~ 4000 and ~ 2500 cps obtained on 0.5 and 2.5 h treated material. This TL reduction effect obtained under air and nitrogen treatment suggests that the trap density of the multiple trap system decrease is mainly driven by the thermal treatment and not by the actual presence of oxygen.

(iii) In contrast to the thermal treatment in air, the thermal treatment in nitrogen does not result in the occurrence of the high temperature TL peak at -30°C.

As an extension of the annealing series under nitrogen discussed so far, the treated U771 sample, was further thermally treated under nitrogen at 700°C for 2 h. After the measurements of excitation spectrum and the TL glow curves with different heating rates the material was further exposed to a reducing atmosphere, i.e. a hydrogen/nitrogen mixture at an elevated temperature of 700°C for 2 h. Again the excitation spectrum and the TL glow curves were measured afterwards.

While the treatment in nitrogen atmosphere up to 500°C influences the light output properties only slightly, a treatment at 700°C reduces the light output substantially over the complete investigated wavelength range. This is in line with the observation that the BAM lattice is not thermodynamically stable above 700°C [16], i.e. such a thermal treatment results in the formation of secondary phases and thus in a reduction of the light output, independent on the excitation wavelength.

The corresponding glow curves measured with a heating rate of 37 K/min are summarised in Fig. 10.

Although the VUV efficiency decreases due to the thermal treatment at 700°C, the decrease of the TL-intensity continues, resulting in vanishing of

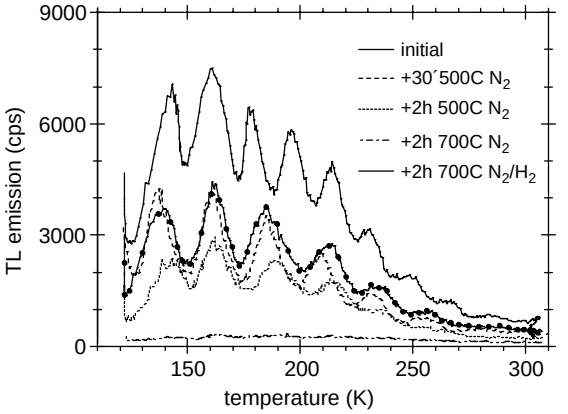

Fig. 10. Development TL glow curves of the BAM:Eu samples due to thermal treatment in nitrogen atmosphere—starting from the initial material (solid) the treatment time and temperature increase successively. The solid line curve with dots is obtained after a additional treatment in hydrogen/nitrogen atmosphere at 700°C for 2 h.

the thermoluminescence signals. Relating the TL-intensity to the trap density means that after the 700°C treatment the initially existing traps are more or less completely removed.

The subsequent high temperature treatment in a reducing H_2/N_2-atmosphere restores almost completely the optical performance in terms of light output but also creates traps as initially present with a density similar to the initial material 30 min treated at 500°C (see dashed and dotted curve in Fig. 10). This observation is in line with the presence of oxygen vacancies in the conduction layer, i.e. in the Ba–O layer, which are spacing the spinel blocks, in β-alumina type host lattices like BAM.

5. Discussion

5.1. Electronic structure of the traps

In general two different models for energetic positions of the trap levels in inorganic solids are discussed [15]:

The first model is based on shallow traps located below the conduction band, whereby thermal activation of trapped electrons results in the release and diffusion of electrons to the activator via the conduction band. The second model is based on trap states located in the band gap, energetically below the excited state of the recombination centre. Because the recombination centre and the traps are spatially localised and the recombination takes place without a transition of the electron into the conduction band, these processes are referred to as localised transitions [6].

As already mentioned, TL is also observed after excitation with radiation energies lower than the band gap of BAM, which is only in line with an electronic trap structure corresponding to the second model with localised transitions (Fig. 4).

This model is confirmed by the fact that the experimentally determined frequency factors are very small, viz. in the order of 10^2 to a few 10^4 s^{-1}. While conduction band related transitions usually exhibit frequency factors of 10^{10}–10^{12} s^{-1}, such very small frequency factors are typical for localised transitions [6]. This small frequency factors are caused by the fact that the relative recombination probability of localised transition is related to the wave function overlap between the trap and the recombination centre.

In Fig. 11 a localised transition scheme is depicted which is in line with all results gained from the TL experiments. The trap states are spatially localised and are energetically below the lowest crystal field component of the excited $4f^6 5d^1$ state (visualised in the scheme by the dotted line) of Eu^{2+}.

In this model the traps in the band gap can also be occupied by applying radiation with energy well below the band gap energy as in the experiments. The resonant TL behaviour occurring at excitation energies matching the energy gap between the valence and the conduction band can be explained by a reduced mobility of the electron-hole pairs energetically positioned at the lower band edge of the conduction band. These electron-hole pairs are more effectively trapped by lattice defects than those being energetically high above the band edge. This also explains the 170 nm peak in the excitation spectrum of undoped BAM (Fig. 1), indicating an efficient exciton trapping by the lattice defects.

The observation, that the excitation of BAM with an energy distinctly higher than the band gap,

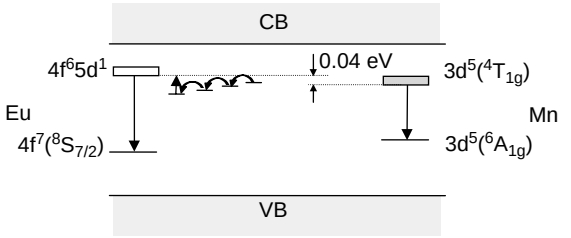

Fig. 11. Localised transition scheme for recombination incorporating spatially localised excitation states and different trap levels. In BAM:Eu the recombination centres are the activator Eu^{2+}, which relaxes due to a $4f^6 5d^1$–$4f^7(^8S_{7/2})$ transition located at 453 nm. The recombination centres in BAM:Mn are the Mn^{2+} ions atoms which relaxes due to a $3d^5(^4T_{1g})$–$3d^5(^6A_{1g})$ transition located at 515 nm.

results in less thermoluminescence, can be explained by an increase in the density of higher Eu^{2+} states, resulting in an enhanced transfer efficiency to the recombination centre Eu^{2+}, by circumventing the trapping states.

If BAM is doped by Mn^{2+} similar glow curves have been obtained proofing that the traps are host lattice related and not specific to the applied activator. As shown before, the analysis of the trap depth energies for Mn^{2+} doped material reveals values $\sim$0.04 eV below the trap depth energies determined for the Eu^{2+} doped material. This suggest that in this lattice the lowest excited $3d^5(^4T_{1g})$ state of Mn is shifted by 0.04 eV with respect to the lowest crystal field component of the excited $4f^6 5d^1$ state of Eu^{2+}.

The defect density of BAM crystals is relatively high, since the integral intensity of the glow peaks are rather high, viz. about ten times higher than for other PDP phosphors, e.g. Willemite Zn_2SiO_4: Mn. It is also confirmed by the relatively intense defect luminescence of undoped BAM crystals (Fig. 1).

The presence of a high concentration of defects in BAM crystals is in line with the observation that even a tiny deviation from the ideal composition during BAM synthesis, results in the formation of impurities, e.g. the β-alumina phase $Ba_{0.75}Al_{11}O_{17.25}$, which is an oxygen deficient composition [17]. Therefore, the shallow traps are assigned to oxygen vacancies, located in the conduction layers of BAM, which is well established as the source of the high ion conductivity of β-alumina [18]. There is proof for the oxygen from the annealing experiments discussed in the next paragraph.

5.2. Annealing of BAM:Eu

The thermal treatment of BAM:Eu in air at 500°C has two effects on its TL spectrum. On the one hand the intensity of the glow peaks related to the shallow traps is reduced and on the other a new glow peak shows up, that is 0.3 eV located below the excited state of the recombination centre. This effect is accompanied by a reduction of the VUV efficiency of BAM:Eu. The high-temperature peak does not appear if BAM:Eu is annealed under nitrogen, while the intensity of the glow peaks related to the shallow traps is still reduced. The intensity of the glow peaks originating from the shallow traps rises again, if a BAM:Eu sample already heated in air or nitrogen is then subsequently annealed in a reducing atmosphere, e.g. in nitrogen/hydrogen. The reduction of the shallow traps can be explained by their assignment to oxygen vacancies (V_O^{**}) in the conduction (Ba–O) layer of the BAM structure. Since the mobility of ions in the conduction layer is rather high, the oxygen vacancies are also relatively mobile.

$$2\,Eu_{Ba}^{x} + 1/2\,O_2 + V_O^{**} \rightarrow O_O^{x} + 2\,Eu_{Ba}^{*}.$$

In other words, the concentration of oxygen vacancies is reduced by the post-annealing step in air due to the Eu^{2+} oxidation accompanied by oxygen diffusion into the conduction layer or by diffusion from oxygen ions from the spinel blocks into the conduction layer.

The reduction of the VUV light output caused by the oxidation of Eu^{2+} to Eu^{3+} (Eu_{Ba}^{x} to Eu_{Ba}^{*}) occurs mainly at the surface of the BAM:Eu particles. The formation of Eu^{3+} at the surface probably causes the high temperature glow peak, energetically located 0.3 eV below the recombination centre. This is confirmed by the observation that this glow peak is not observed after annealing of BAM:Eu in nitrogen at 500°C. In this case, only the concentration of the oxygen vacancies is reduced by thermally activated diffusion, i.e.

diffusion of oxygen ions on interstitial sites to anion vacancies.

$$V_O^{**} + O_I \rightarrow O_O^x.$$

The remaining defect states completely disappear if a BAM:Eu sample is exposed to an additional annealing step at 700°C under nitrogen. This process is accompanied by a reduction of the concentration of Eu^{2+} or by the decomposition of the BAM phase, since annealing at 700°C also reduces the VUV and UV-C efficiency. This explanation is confirmed by the decrease of the absorption of Eu^{2+} derived from diffuse reflection spectra.

The oxygen vacancies in the conduction layer of BAM are probably caused by the application of a reducing atmosphere during BAM synthesis, that is required to reduce Eu^{3+} (starting material is Eu_2O_3) to Eu^{2+} . The application of a reducing atmosphere during the synthesis of BAM or during a post-annealing step, results besides the reduction of Eu^{3+} also in the removal of some oxygen atoms from the lattice (reduction), leading again to oxygen vacancies in the lattice.

$$2\,Eu_{Ba}^x + H_2 + O_O^x \rightarrow H_2O + V_O^{**} + 2\,Eu_{Ba}^*.$$

This was proven by the observation that the "defect free" BAM sample obtained after the annealing at 700°C in nitrogen shows the same glow peak structure in the TL spectrum after an additional thermal treatment under nitrogen/hydrogen.

6. Summary and conclusions

The defect structure of Eu^{2+} and Mn^{2+} doped BAM was determined by means of thermoluminescence spectroscopy. The glow curves revealed that BAM comprises several shallow traps, located 0.1–0.2 eV below the recombination centre. It was demonstrated that the type of activator does not affect the energetic position of the traps in the band gap of BAM.

By the investigation of BAM:Eu samples, thermally treated in air or nitrogen, it was elucidated that the concentration of the shallow traps decreases with increasing annealing time. By annealing of "defect free" BAM in nitrogen/hydrogen the shallow traps can be recovered, which is caused by the removal of oxygen from the conduction layers in BAM, leaving oxygen vacancies behind. The shallow traps have hardly any impact on the VUV efficiency.

In contrast, the oxidative thermal treatment of BAM results in a reduction of its VUV efficiency which has also been observed in PDP manufacturing. This oxidation is accompanied by the formation of a deeper trap at 0.3 eV below the recombination centre. Therefore the presence and the intensity of this glow peak is a useful measure to estimate the degradation of BAM:Eu during a device production step including thermal treatment.

Since the deep trap disappears after an additional thermal treatment in a reducing atmosphere, it is recommended to apply such a treatment to recover the VUV efficiency of BAM:Eu.

Acknowledgements

The authors are grateful to Prof. Dr. M. Goebbels for the fruitful discussions concerning the BAM structure and to Dr. D. Bertram for the critical review of the manuscript.

References

[1] T. Jüstel, H. Bechtel, H. Nikol, C.R. Ronda, D.U. Wiechert, Proceedings of the Seventh International Symposium on Physics and Chemistry of Luminiscent Materials, 1998, p. 103.
[2] S. Oshio, T. Matsuoka, S. Tanaka, H. Kobayashi, J. Electrochem. Soc. 145 (1998) 3903.
[3] M. Ilmer, S. Kotter, H. Schweizer, M. Seibold, Proceedings of IDW'99, 1999, p. 65.
[4] A.L. Diaz, C.F. Chenot, B.G. deBoer, Proceedings of Eurodisplay, 1999, p. 65.
[5] M. Zachau, D. Schmidt, U. Mueller, C.F. Chenot, 1999, WO 99/34389.
[6] R. Chen, S.W.S. McKeever, Theory of Thermoluminescence and Related Phenomena, World Scientific Publishers, Singapore, London, Hong Kong, 1997.
[7] J.T. Randall, M.H.F. Wilkens, Proc. R. Soc. London 184 (1945) 366.
[8] J.T. Randall, M.H.F. Wilkens, Proc. R. Soc. London 184 (1945) 390.

[9] R.H. Bube, Photoconductivity of Solids, Wiley, New York, 1960.
[10] D.R. Vij, Luminescence of Solids, Plenum Press, New York, 1978.
[11] P. Kivits, H.J.L. Hagebeuk, J. Lumin. 15 (1977) 1.
[12] W. Hoogenstraaten, Philips Res. Rep. 13 (1958) 515.
[13] R. Chen, S.A. Winer, J. Appl. Phys. 41 (19) 5227.
[14] T. Jüstel, J.-C. Krupa, D.U. Wiechert, J. Lumin. 93 (2001) 179.
[15] N. Iyi, S. Takekawa, S. Kimura, J. Solid State Chem. 83 (1989) 8.
[16] S. Shionoya, W.M. Yen, Phosphor Handbook, CRC Press, Boca Raton, 1999, p. 92.
[17] M. Göbbels, S. Kimura, E. Woermann, J. Solid State Chem. 136 (1998) 253.
[18] A.R. West, Solid State Chemistry, VCH, Weinheim, 1992.